



TEA Systems Corporation  
65 Schlossburg St.  
Alburtis, PA 18011 USA

Phone: (+01) 610 682 4146  
Email: [Info@TEAsystems.com](mailto:Info@TEAsystems.com)  
<http://www.teasystems.com>

## Full sub-65 nm data-modeling for Photomask Manufacturing and the benefits derived in device fabrication

Terrence E. Zavec<sup>\*</sup>  
TEA Systems Corporation

**KeyWords:** DFM, OPC, ACLV, empirical, profile, simulation, IsoFocal Bias, Wafer Bias, Dose Uniformity, Reticle, Mask, Process Control, Design, Manufacturing Control, Lithography, Metrology

### 1. Abstract

Advanced mask designs link the design corrections on a reticle to the image perturbation signatures of the end-user in the final design stages of the reticle structures. Since any reticle must be created before the first silicon exposures are conducted, the major burden of specification for the process-active elements of the reticle has been relegated to simulation. Simulation complexity has grown to meet this need from the software-only, small area simulations of a few microns to recent hardware-enhanced full-field simulation of the reticle.

Full-field simulation also has progressed from an unlinked, first-principles wavefront construction to include the first steps in providing real-process boundary conditions. This calibration to the process uses a limited set of feature-width metrology taken from a focus-exposure matrix to perform a classic “process window” calculation of process response from techniques developed over three decades ago. The benefits that could be gathered from recent advances in full-profile process metrology are ignored.

We present a new method for a comparative characterization of advanced reticle structure design based upon their response to a wafer-facilities specific set of tool and process interactions. These characterizations can be used for calibration of the simulation for a user-specific process or for a precise comparative evaluation of optical proximity structure design alternatives. This technique advances beyond the classic methods of process window calculation by applying multi-layered physical response models that deconvolve perturbation signatures of the tool sets and processes involved in imaging the reticle on the wafer.

Wafer Bias of the reticle-to-wafer sequence is derived and used as the variable for this analysis. The design structures on the reticle are shown to exhibit both a static perturbation signature as well as a dynamic component that is sensitive to localized process conditions on the wafer. Finally the components contributing to wafer bias for the process under study are deconvolved to show both the stability of their error signatures and relative significance to a quantitative determination of specific OPC structure robustness to process variance.

### 2. Introduction

If the precision and relative accuracy of the Photomask Facility’s toolset contains sufficient process margin then production yields can be efficiently controlled using statistical methods. It’s simply a matter of gathering the data and confirming the proper operation of each metrology and patterning tool using maintenance procedures. However these simpler times are gone when device designs enter the realm of the sub-65 nm design rule reticle set. To meet these new challenges the industry needs to tune the Photomask Facility’s Optical Proximity Correction (OPC) simulation tools and fabrication processes to the anticipated interactions of the reticle image as it is perturbed during imaging on the wafer.

---

<sup>\*</sup> Contact: [tzavec@TEAsystems.com](mailto:tzavec@TEAsystems.com) phone: (+01) 610 682 4146, <http://www.TEAsystems.com>

Recent introductions of commercial, hardware-enhanced simulators are used to optimize the full-field image in order to reduce costly feature-enhancement mistakes during design. These simulations have taken the first few steps to apply real-world boundary conditions to their calculations by incorporating a calibration to the process excursions measured across the customer's process using focus-exposure matrices and the classic "process window" analysis. Yet these methods do not consider the additional significant process and toolset specific signatures of the end-customer.<sup>1</sup>

Recently awareness has risen for the need to verify both overly and etch-depth during Phase Shift Mask (PSM) manufacture. Here we see a need to bias phase shift etch-depth parameters away from their theoretical design targets to compensate for "unknown" biases that are in fact systematic process and tool errors<sup>2</sup>. The considerations studied in these papers neglect the full final response in the customer wafer fab. The studies also neglect to link the wafer processes true feature-profile response to the individual site-signatures of the mask by relying solely on arbitrary width measurement of profiles.

If a precise analysis were available that could carefully model the spatial distributions of the feature profiles, it could then also extract process signatures and a detailed mask response to them. The coefficients of the modeled process signature could be used to stabilize and tune production in both photomask and end-customer device manufacturing and therefore optimize final device yields and minimize the time required to achieve optimum yield for new processes.

What is lacking is the proper analytical toolset to perform this link between the simulation optimized OPC photomask and the process signatures of the wafer and photomask process. Process window comparative evaluations assume a response model first presented 3 decades ago. A comparison of individual OPC structure responses using classic process window techniques does not have the resolution to determine the performance and response of the process to small changes in design. The linkage must be capable of providing a direct and clear comparison of reticle-structure design option performance as well as accurate calibration metrics for the structure's design simulator.

The resolution of this problem lies in the ability of new metrology technology to quantitatively and accurately measures the full profile of the actinic film stack of a wafer exposure. New analysis techniques are needed to take advantage of this full-profile characterization.

We present here a direct and conceptually simple approach to improve the evaluation of OPC designs using multi-layer empirical data modeling of the imaging process. The method is illustrated by an analysis of the variance of reticle-to-wafer bias based on metrology gathered from both reticle and wafer profiles. While the wafer bias variable is used as a demonstration vehicle for the method, any profile variable could be used with equal precision.

### 3. Experimental Setup

Data for this analysis was gathered from 90 and 60 nm structures setup on a phase shift test reticle. The reticles were fabricated in both Chrome/Chrome-Oxide and MoSiON or "Moly" substrates.

Substrates were exposed on 193 nm wavelength scanners using 0.75 NA. The reticles were measured using Hitachi S9260 CD-SEM and Nanometrics Atlas metrology tools for reticle and wafer. Analysis of the data and charts were created using TEA Systems Weir PW and Weir ProMEEF software.

### 4. Signatures and Simulations

The design of a Reticle Enhancement Technology (RET) mask is complicated by the fact that the final image cannot be directly correlated to the features on the reticle. Optical Proximity Correction (OPC) phase shift structures are strongly influenced by the characteristics and uniformity of the phase-shifting elements. Other methods such as the Inverse Lithography reticle designs such as shown in figure 1, bear even less resemblance to the structures that will eventually be encapsulated into the photoresist image on the wafer.

Process Simulators are used to calculate image formation within the photoresist. The most basic simulators consider the effects of photoresist thickness, absorption, materials and processes of the company. The effects include the active processes of the photoresist from exposure of the photoactive

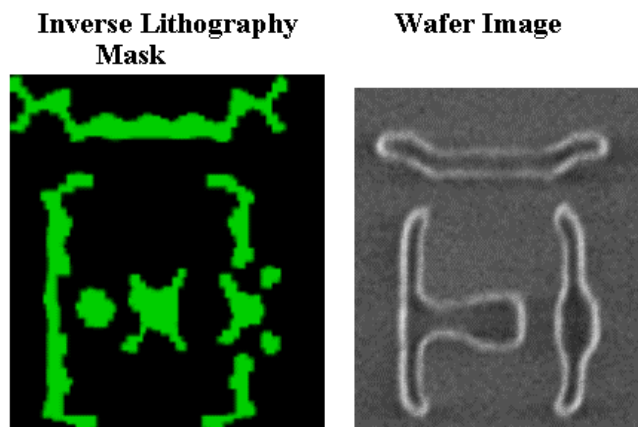


**Figure 1:** Reticle enhancement replication on the wafer is not intuitive. (Courtesy Luminescent Technologies)

**Left:** Design layout for transistor gate structure on reticle

**Right:** Image in photoresist on the wafer.

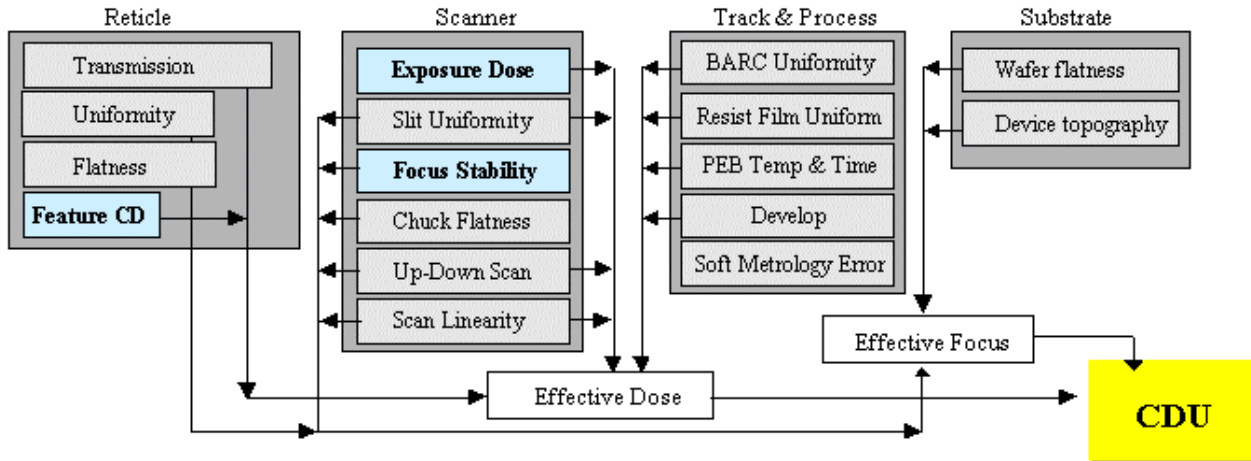


**Figure 2:** Perturbation sources of Critical Dimension Uniformity (CDU)

component, reaction, amplification and diffusion during the post-exposure bake. Advanced systems consider some optical aberrations and others will add Hyper NA, immersion lithography and polarization characterization. Structures are simulated over a small area of the photomask of about 50 to 100 microns without any direct linkage to the actual image on the wafer for boundary calibration.

Recent hardware-accelerated systems can simulate larger areas of the chip with limited linkage to the process setup variables of focus and dose. Three or four sites in a focus-exposure matrix (FEM) are tested to provide the most basic of boundary conditions for the simulation. All other parameters in the model, including those related to the mask, optics, resist, film, scan and etch are assumed to remain constant across the entire window of the process.

During calibration the simulator relies upon a computational lithography model using first principle rigorous electromagnetic field simulation of polarization and scattering caused by features on the photomask. Software-based simulators frequently make approximations to shorten the calculation time while hardware-enhanced offerings offer more rigorous computation that shortens the calculations to several hours.

While the most-advanced simulators calibrate to a few focus/dose settings, none account for the twenty-two major sources of variation shown in figure 2<sup>3</sup>. Calibrating several focus and exposure data points to a single point in the exposure field ignores the impact of all the perturbations shown in figure 2 including the effective dose uniformity and focus stability of the exposure tool.

The simple “process-window” analysis that is used for setup and calibration only approximates the true response interactions of the exposure tool, reticle and process. OPC simulator calibrations incorporating the simple setup are subject to soft metrology errors as well as localized variations in exposure and exposure tool perturbations that may differ significantly from those tested under the sparse sampling involved. These localized variations represent significant and stable perturbation signatures of the process that combine to create the final photoresist image.

State of the art for “process-window” calculation continues to follow the basic model for photoresist interactions first presented by John Bossung in 1977<sup>4</sup>. This is a simplified interaction concept that has had several thousand papers reference it over the years and no significant improvements have been implemented since its inception. It is inconceivable that an algorithm constructed for the technology of that era and not referencing the basic physics of the process could still be relied upon as the major empirical control method for the setup and characterization of today’s complex processes.

A wide selection of process-window tools is available today. They are all based upon Bossung’s original work and differ only in the manner of their regression. Their major drawback is that they are nothing more than a polynomial expansion used to explain the predominant observations of focus and dose on a feature width. Their use is highly subjective and results vary significantly with the location of the measurement on the profile and the profiles location in the exposure field. The process window method begins to break down when more than one feature type is examined. The results obtained grow even more obtuse when trying to account for the variations seen for multiple points across an exposure field due to the cross interactions of lens aberrations and the process film stack.

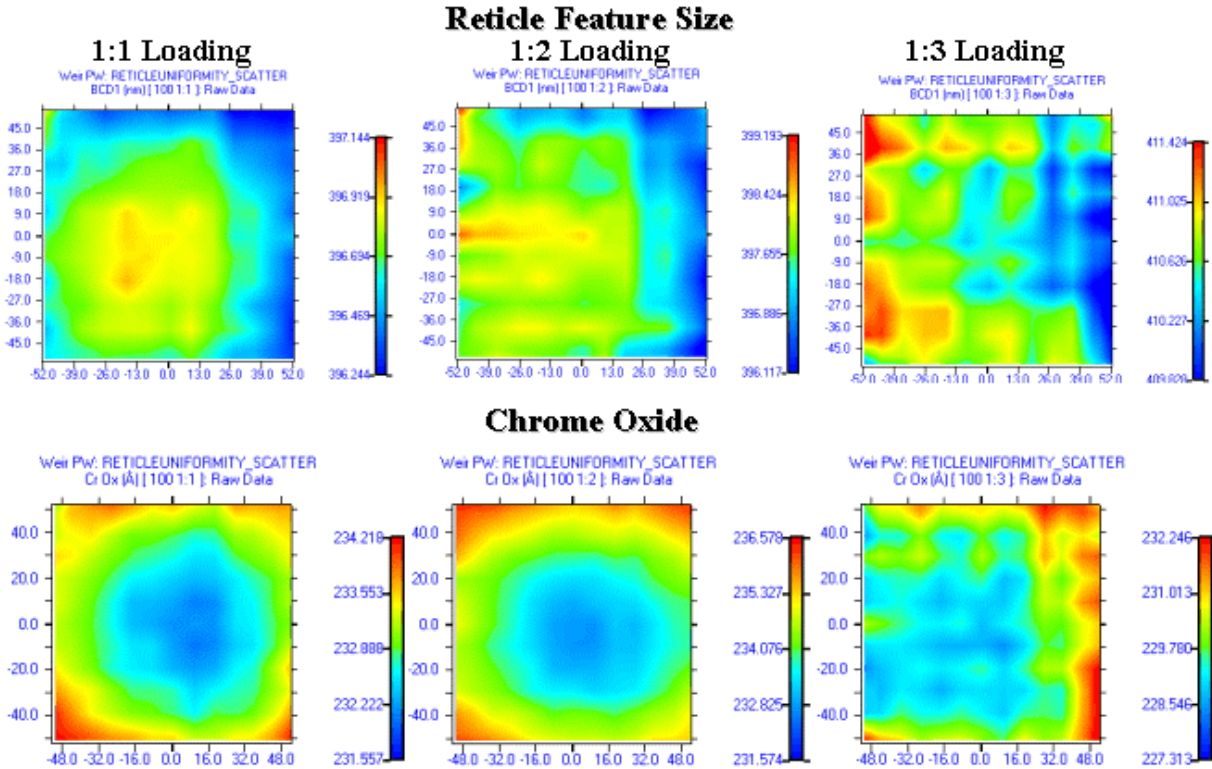


Figure 3: Cr Ox film and feature (BCD1) uniformity across a reticle for 1:1, 1:2 and 1:3 pattern loading

### 5. Reticle Signatures in the Process

Optical Scatterometry (OCD) tools are now capable of measuring 4:1 reticles with features used in sub-90 nm node lithography.<sup>5</sup> As a first part of the experiment we examined a 400 nm design-size reticle feature, 100 nm wafer size, which was contained in targets with 100 nm, 200 nm and 300 nm period structures to evaluate dense (1:1) to isolated (1:3) feature response. The features were directly measured with the Nanometrics Atlas M and their characteristics studied using TEA System’s Weir PW. The contour plot of figure 3 shows both the feature size (BCD) and Chrome-Oxide (Cr Ox) uniformity of an 11 x 11 matrix of measurements taken across the reticle for each structure. The feature-measurements of the reticle comprise the elements “Static” signature. These directly measured values form a base behavioral element that responds to wafer exposure in the classic manner. The static signature can be perturbed by many elements including variations in reticle bow and tilt introduced during exposure.

The Moly and Cr Ox film nonuniformity engenders a response that is dynamic in nature when considering it’s influence of wafer exposure. Notice that the radial symmetry of the measured Chrome Oxide for the 1:1 and 1:2 periodic structures shown in the bottom of figure 3. This symmetry disappears when the “1:3” or 300 nm period isolated structures are measured. Feature size signatures track those of the Chrome Oxide with an obvious physical transition that follows the design progression from dense to isolated.

As mask-makers have recognized for many years, features with a periodicity of less than 1.3x their feature size exhibit proximity effects. What is interesting here are the coupling of feature size with the Chrome Oxide thickness and the differences seen in uniformity.

The radial symmetry of the dense structures in CrOx film is also

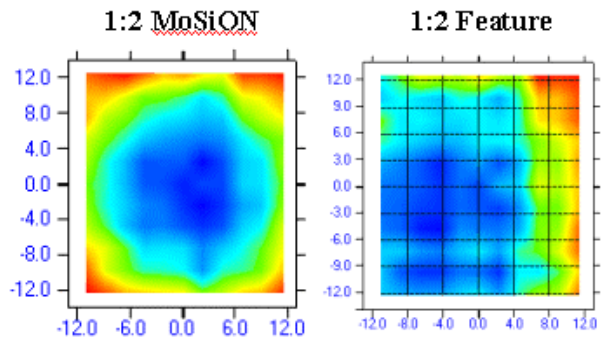
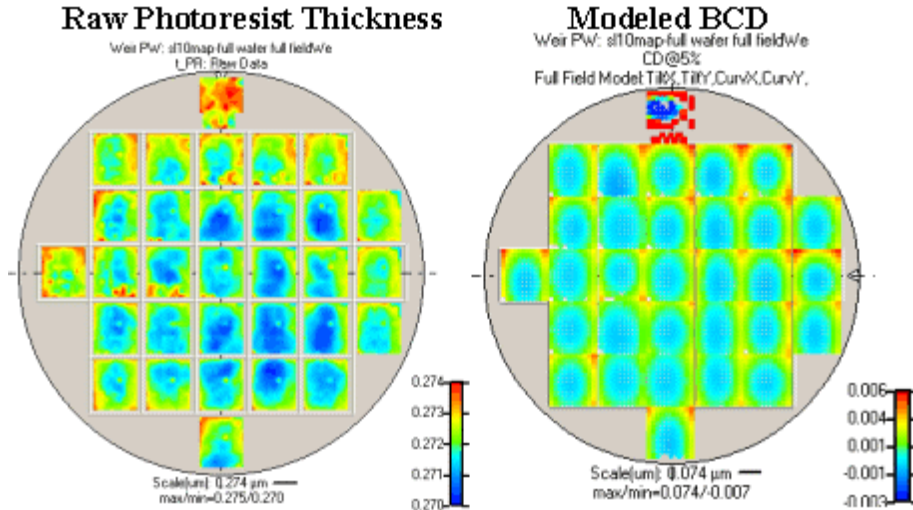


Figure 4: MoSiON Reticle film and feature uniformity  
Left: MoSiON uniformity on a reticle for a 1:2 dense packed periodic structure of 400 nm  
Right: Feature size uniformity



**Figure 5:** Raw photoresist thickness (left) and radial-modeled field perturbations (right) for Bottom Critical Dimension Features.

seen in the Moly reticle’s MoSiON uniformity shown in figure 4 for 1:2 dense structures. The film and critical feature uniformity in this case are not as similar as in figure 3. The feature signatures for this reticle has been shown in previous publications to be traceable within 1 nm between SEM and OCD measured reticles and for resist images on the wafer.<sup>5</sup>

A scan model of feature-widths from wafer data replicates the reticle signature observed on the right side of figure 4. To observe the contribution of this Moly film signature to it’s the wafer image we applied one of the Weir PW radial symmetry models to every field on the wafer. This model looks for radial symmetry about the center of the exposure field and yields the contour plots shown in figure 5. Photoresist thickness is known to change with effective dose and the Moly signature of figure 4 is clearly evident in the contour plot of every field’s photoresist thickness on the left plot of figure 5.

Even more interesting is the modeled symmetry of the bottom of the critical dimension (BCD) profile measurements shown on the right side of figure 5. This plot examines only the first (TiltX, TiltY) and second (CurvX, CurvY) order coefficients of the radial symmetry model, field-to-field offsets and higher orders are neglected. Here again the symmetric reticle’s Moly signature appears as a perturbation source for the BCD feature accounting for 4.5 nm of variation. Film uniformity on the reticle is therefore a critical issue in the full-field feature uniformity budget.

If wafer bias is to be calculated, then the reticle values for every feature must be measured and stored as the tools signature. The impact of reticle film uniformity on final feature size varies with the type of reticle as well as the size and density of the feature exposed relative to the actinic wavelength of the exposure.

## 6. Soft Errors in Metrology Data

Another factor that enters into consideration when calculating wafer-bias of a reticle is the influence of soft errors in the metrology data.

Soft errors are sinister when calculating wafer bias or when modeling any process response. They do not reflect the real process response of the feature and are easily overlooked unless the user or software is not keenly aware of the proper systematic response that must be present in across-wafer, field or focus-dose data surfaces. When present they can strongly bias regression modeling of the response unless they are detected and removed beforehand.

Metrology tools, Scanning Electron Microscopes (SEMs) in particular, often capture a near-neighbor of the feature rather than the intended feature. This occurs most often for structures

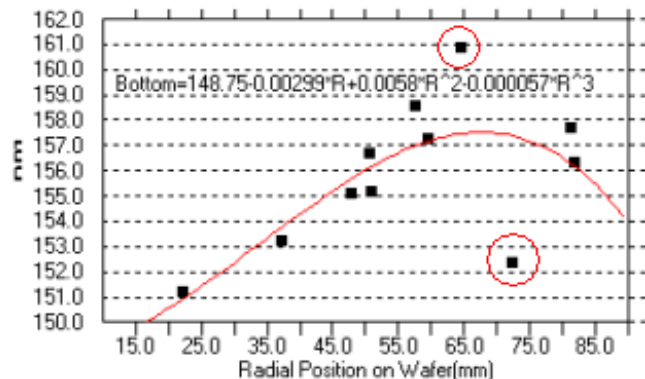


**Figure 6:** Soft errors in the raw metrology data (circled)

that are dense packed with the nearest features lying closer than 1.3x the size of the feature (i.e. 1:3 loading).

An example of how a metrology tool can result in “soft” biasing of the true feature performance can be seen in figure 6. The data in figure 6 is CD-SEM data taken from a wafer with a symmetric Anti Reflective Coating nonuniformity. In this graph a sub-65 nm feature’s end-gap is measured to the next nearest feature that by design is a 150 nm gap. Gap data in figure 6 is plotted by Weir PW as a function of each point’s radial position from wafer-center. The two encircled points represent measurements taken by the SEM on the wrong section of the feature. If these points are not excluded from the data during the fit-process the resulting coefficients will not be properly calculated.

Soft errors in metrology most frequently result from improperly captured target locations. Errors occur in regions where imaging is less than optimal such as those regions where the feature size and loading approaches the resolution limits of the exposure tool. This study found that while soft errors occur in all metrology, CD-SEM metrology is more apt to exhibit soft errors because of the uncertainty created by charging from repeated scans, scan averaging into areas not representative of the feature and the overall small area of measurement on the feature.

Data culling must maintain an awareness of the overall characteristics of the sub-population such as their location on the wafer, field or within a focus-dose array. We found that these errors could be detected by pre-sorting the data into the population subset needed for each section of the calculations. A comparison of the data against the distribution of the majority of the sub-population was sufficient to detect and remove soft metrology errors. For the example shown in figure 6, the data response as a function of it’s distance from the wafer center was collected and fitted to the model. Each point is tested against its residual value.

### 7. Calculation and Modeling of Wafer Bias

Mask feature profiles were measured in an 11 by 11 array on the MoSiON reticle using both the Hitachi CD-SEM and Nanometrics Atlas M Scatterometer. Wafers were then exposed in a focus-exposure matrix and data measured in a 7 by 11 array using another Nanometrics Scatterometer.

TEA Systems Weir ProMEEF software was used to align, scale and rotate the reticle data to fit the proper wafer sites. Since the measured arrays were not on the same stepping, the software used an interpolation model on the reticle sites to properly calculate the closest possible fit. Wafer bias is calculated as a simple difference between the wafer and reticle value for each wafer site. The Wafer Bias data is then used by Weir PW to model systematic variations across the wafer and field. A contour plot of the FEM for feature-bottoms of a vertical 90 nm feature is shown in figure 7. This wafer was exposed with a 193 nm wavelength scanner at 0.76 NA. The array of the contour plot is zeroed at 0 um defocus with steps of +/- 0.05 um. Dose ranged from 19 to 25 mj/cm<sup>2</sup>.

Bias in figure 7 averages about -16 nm for the FEM. The presence of across-die Wafer Bias nonuniformity is evident in this raw data. We therefore modeled both the slit and reticle-scan response of every field on the wafer. Our field-composite model of perturbation consists of separate slit and scan components that follow the form:

$$IF_p(x,y) = IF_{slit} + IF_{scan} + IF_{reticle} + r \quad (1)$$

Where  $IF_p(xy)$  is the IntraField component of the of the profile describing both the feature profile and it’s perturbation response for every slit ( $IF_{slit}$ ) and scan ( $IF_{scan}$ ) position on the field.<sup>6</sup>

The  $IF_{reticle}$  static signature for this application has already been removed with the calculation of the Wafer Bias. Any systematic variation from the reticle will be from film nonuniformity or other process variations. Bow or tilt of the reticle as it’s mounted upon the scan stage and exposed from field-to-field will take the form of:

$$IF_{slit} = \sum_{Rows} \sum_{n=0}^4 a_n x^n \quad (2)$$

for the lens slit and

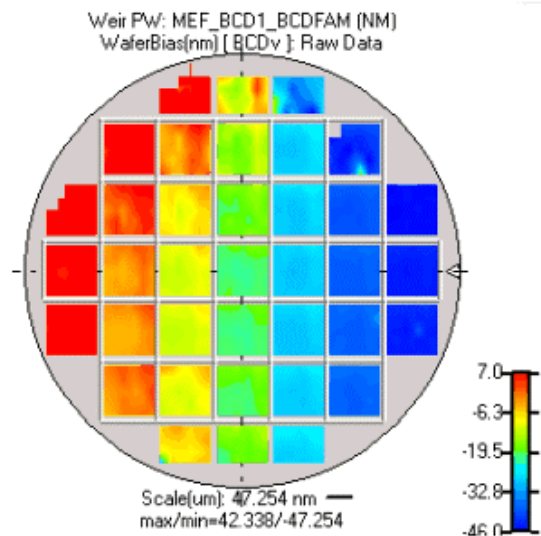


**Figure 7:** Contour plot of wafer bias uniformity across a focus (rows) – exposure (columns) matrix.

$$IF_{Scan} = \sum_{Column=1}^n \sum_{j=0}^4 a_j y^j + r \tag{3}$$

for the reticle scan stage. The “r” designates the residuals to the modeled systematic perturbations. The constant coefficient for Wafer Bias for the full focus-exposure matrix is  $-17.09 \pm 1.25$  nm with fitted and systematic results summarized in Table 1.

**Table 1: Modeled Results of Row-Model fit to FEM**

	Family	Count	Mean	Median	Range	StDev
<b>Systematic</b>	BCDv	1051	-16.62	-6.26	82.52	18.55
<b>Residuals</b>	BCDv	1051	0.00	1.92	37.43	2.43

The results displayed in Table 1 provide an improved calibration for simulation or OPC structure performance comparison. The residuals for this process cover a third of the range of the systematic errors. Recall however that the results shown in Table 1 are for the Slit or “row” model of the field. Reticle-scan and high-frequency errors not detected by equation 2 will appear in the residuals to the regression.

The significance of this model’s coefficients and this methodology is that we now have a data set that accurately describes the systematic response of the image due to both tool and process distortion independent of the static signature of the reticle. Classic process-window surface models force all reticle, exposure tool and process variance into rigid series polynomial of the general form<sup>6</sup>:

$$W = \sum_{m=0}^M \sum_{n=0}^N \alpha_{nm} \left( 1 - \frac{E_s}{E} \right)^n F^m \tag{4}$$

Equation 4 approximates feature size response using only the fixed relations of exposure (E) and Focus (F) as input variables. The structure is rigid and results obtained for best focus and dose are biased by FEM data that extends beyond the process window limits and by thickness variations in the translucent film stack. Variables other than feature size, such as reacted film thickness, side-wall angle and etch depth are not well handled by equation 4. Lens aberrations and the mechanical perturbations introduced by reticle-stage scan, variations in effective dose and reticle distortion result in composite process window results that do not overlap into any realistic representation of the true full-field process response.<sup>7</sup>

The spatial-linked models of equations 2 and 3 replicate the physics of the imaging process without the inaccuracies of the blind polynomial fit of Equation 4.<sup>6,8</sup> The model now directly addresses the systematic variations experienced by each feature for perturbations introduced by the exposure tool and reticle while removing the small high frequency components that comprise uncorrectable scan artifacts and random errors introduced by the exposure and metrology sequence. As will be shown in the next section, the model also provides methods for quantification of these residual artifacts.

## 8. Analysis of the Full-Field Wafer Bias Process Window

Table 1 summarizes the overall process response results for a reticle feature-

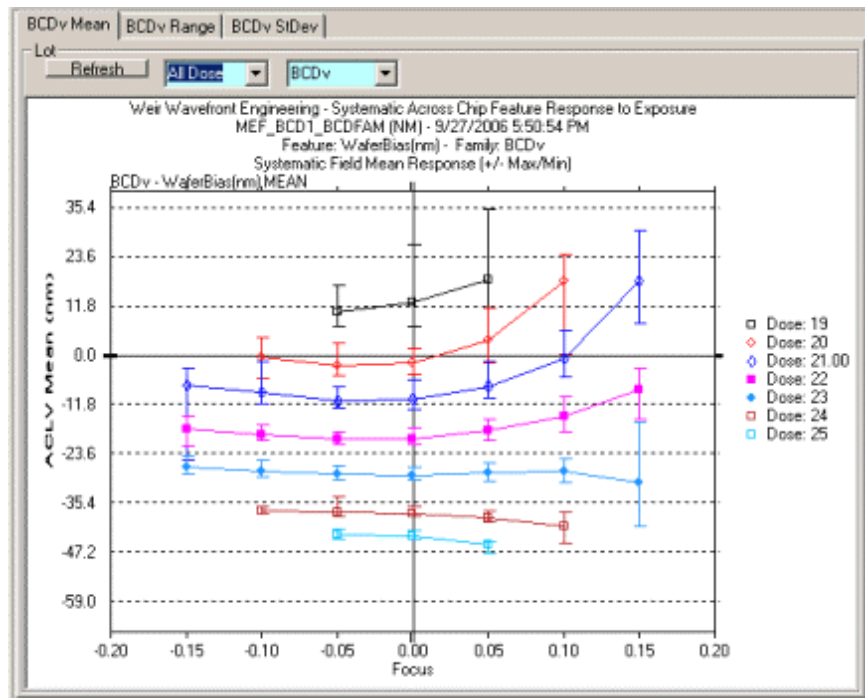


**Figure 8:** Full-Field systematic Wafer Bias response of Bottom CD to Focus.

family, in this case the Bottom CD of Vertical features, for variations across the focus-exposure process window. The systematic variation shows a Bias of  $-16.6$  nm with an uncertainty of the estimate of only  $1.25$  nm. Systematic variation due to exposure and the perturbations of the lithography cell will range in bias by  $82$  nm with a standard deviation of  $18.55$  nm. Residuals to the systematic perturbations form a standard deviation of only  $2.43$  nm for all data in the process. The broad spread of information contained within this analysis of systematic variations can be broken down by an examination of the systematic perturbations.

Systematic perturbations across the scanned-field will change the effective bias along with focus and dose. The dose-curves of Figure 8 plot the systematic field bias response as a function of focus. The “error bars” attached to each point represent the maximum and minimum systematic wafer-bias excursions for each exposure position of the full-field matrix.

Process response can be clearly interpreted from this graph.

- The IsoFocal dose is clearly seen to reside at  $23$  mj/cm<sup>2</sup>.
- The IsoFocal dose results in a bias of  $-30$  nm. This implies that a reduced  $100$  nm  $1:1$  nominal reticle feature size will respond with the least variation if it is biased to  $70$  nm for vertical features and under this process.
- Full field variation in bias is greater for dose values less than the IsoFocal dose. A more robust process response can be achieved when bias meets or exceeds the IsoFocal exposure.
- The full-field variation in bias is asymmetric around the  $-0.025$   $\mu$ m best-focus point. Across Chip Linewidth Variation (ACLV) will be lower and more tolerant of variations if the process window is centered slightly to the negative side of best-focus.

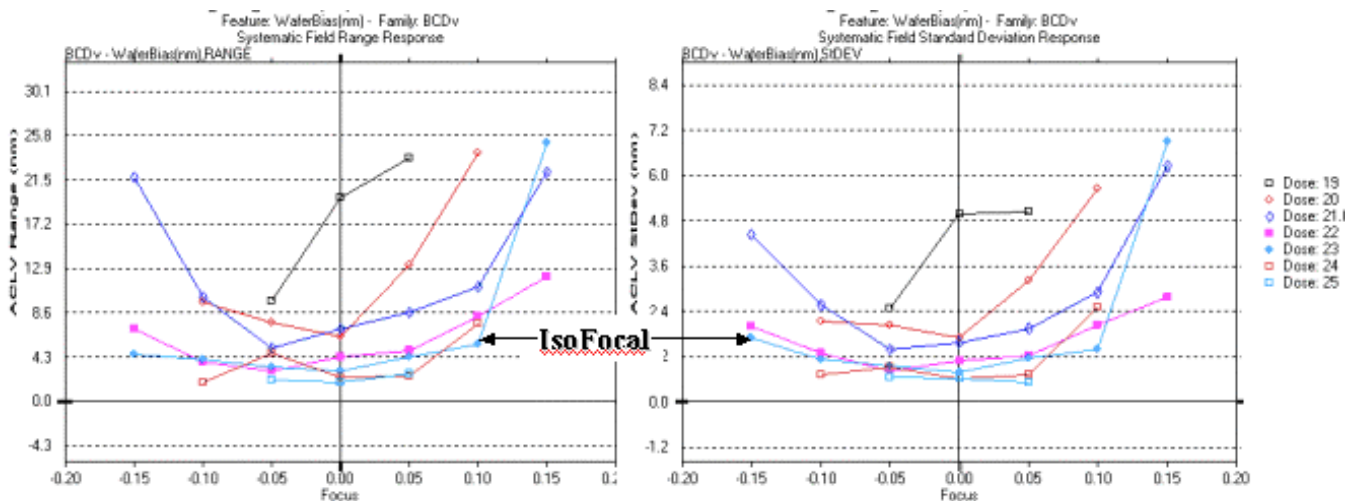
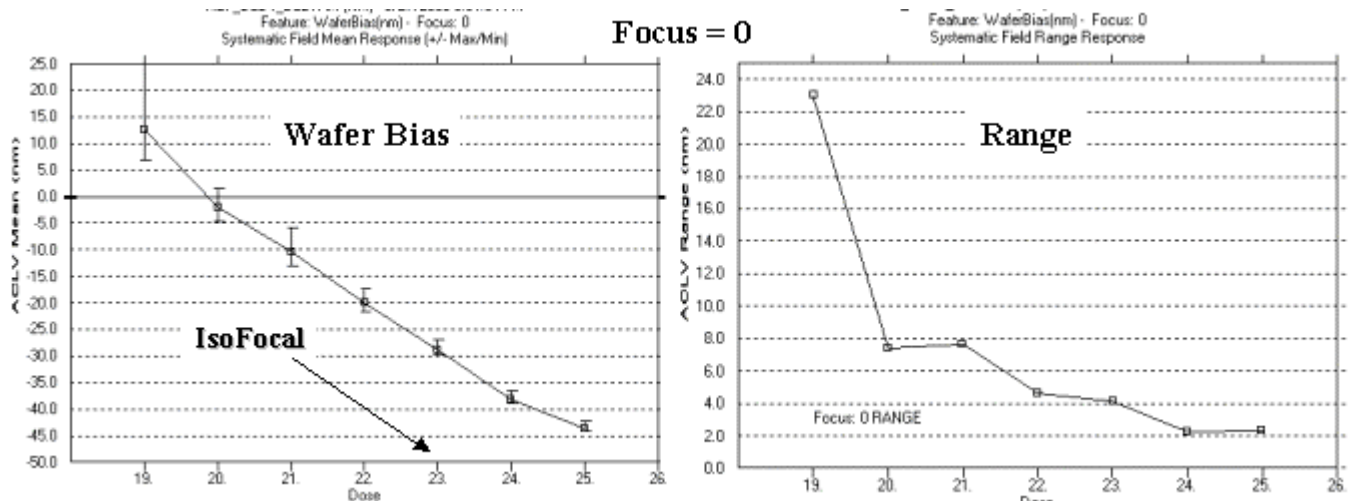


Figure 9: Full-Field systematic Range (left) and Standard Deviation (right) of across-field Wafer Bias variation.

The Range and Standard Deviations (StDev) response of the full-field Wafer Bias can be explored further by an examination of figure 9. The Range of across-field wafer bias exhibits a quadratic response with a minimum centered at best-focus for exposure values near and above the IsoFocal dose. The standard deviation of Wafer Bias variation across the field also varies quadratically about the optimum focus. A clearer vision of this response can be seen in the single-focus curve of figure 10.

Wafer Bias response, for exposures near best-focus as shown in figure 10, is linear with full-field ACLV minimized near the IsoFocal dose, in this case  $23$  mj/cm<sup>2</sup>. The full-field range of bias variation is greater for the underexposed fields as can be seen in the Bias Range graph on the right side of figure 10. A dose difference in only  $2$  mj/cm<sup>2</sup> underexposure can double the ACLV from  $4$  nm to  $8$  nm while overexposed devices exhibit improved uniformity. This implies that reticle designs should be constructed to bias beyond the IsoFocal dose to optimize ACLV uniformity.



**Figure 10:** Wafer Bias response (left) and across-field Range (right) of Wafer Bias at best-focus

The linear range of wafer bias plotted on the left side of figure 10 corresponds to the optimal exposure latitude for the device. In this region the features are in control across the full exposure field. There is some slight reduction in ACLV for dose values less than 22 mJ/cm<sup>2</sup> but no real loss until exposures drop lower than 20 mJ/cm<sup>2</sup>.

### 9. Adjunct Wafer Bias Analyses to the Process Window

A modeled analysis of each exposed row or column for every field of the FEM provides an opportunity to observe the variations in imaging induced by the reticle-scan sequence and lens-slit. For example, figure 11 plots the full wafer bias variation for the FEM with the fitted bias-offset constant coefficient removed from each column of data. A column-model was used for this figure so that by removing the constant value for each fit we essentially removed the across-slit signature for the exposure tool. This technique yields a clearer picture of the bias variations and how they range independent of the features base offsets induced by the exposure tools set focus and dose.

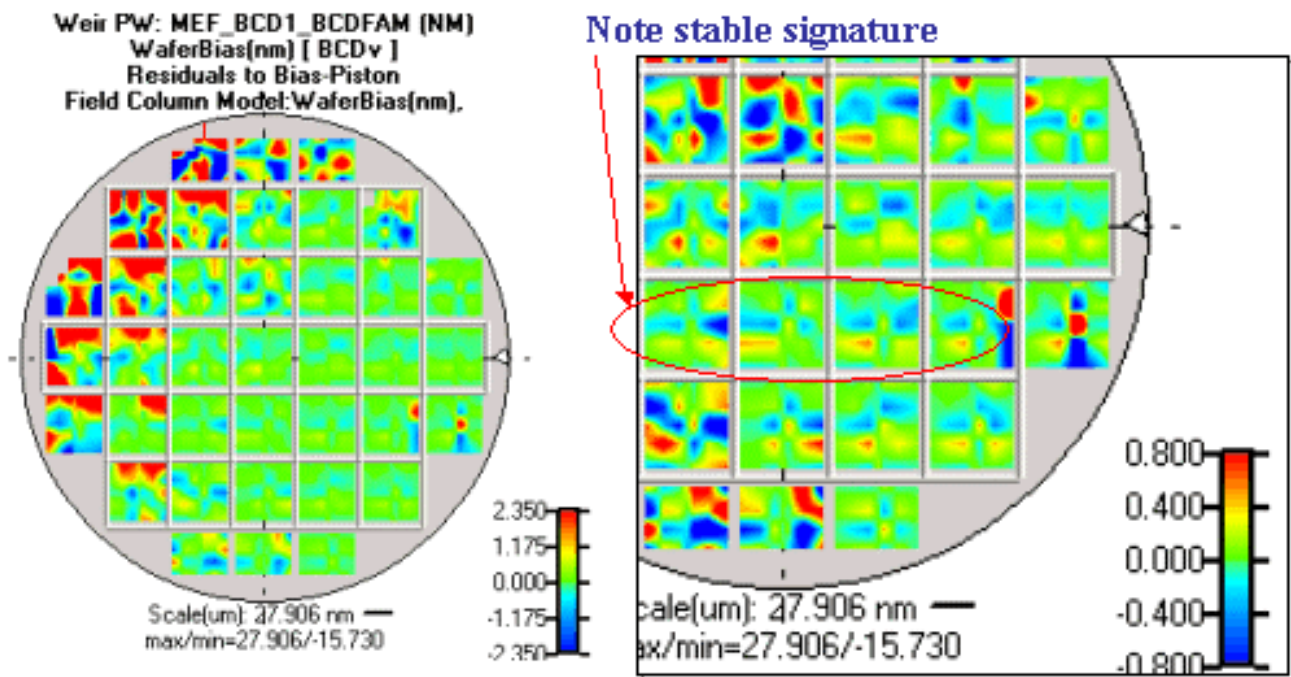


**Figure 11:** Reticle-to-wafer bias of vertical feature bottom measurements with column-model constant coefficient removed.  
 Left: Full wafer showing ACLV without reticle and lens-slit perturbations  
 Right: Magnified view with increased resolution scale of reticle-scan stage induced consistent bias signature.

The wafer plot on the upper left side of figure 11 shows the larger variation in wafer bias seen for the lower dose settings, higher focus values. Notice how the top of each field is particularly susceptible to larger bias values. This behavior can be caused by nonlinearity in the speed of the reticle-stage scan at the top of each field. Keep in mind that the range of bias variation here is 4.7 nm as shown on the calibration bar in the lower right of the plot.

The optimal process window is centered in the range of field plots showing the whole-field area as a green color, this is the area where across-field bias deviation values are very close to zero. A detailed plot of this area is shown on the right side of figure 11 with the plot scale now ranging from +0.8 to -0.8 nm. The lens-slit is shown here to be generating a strongly repetitive signature that is most clearly visible in the four die contained within the red-ellipse. This is a signature that is most likely caused by the travel of the reticle stage during the scan cycle.

There is no detectable sensitivity to reticle scan direction in the FEM data of figure 11 since we removed the constant coefficient from every model. Reticle stage scan direction is often a contributor to bias variation and is highly susceptible to tool setup. An example of scan direction bias sensitivity was obtained from a fixed focus/dose wafer for the data plotted in figure 12.

The exposure-row at the bottom of figure 12 contains the contours for those fields located across the center row of the wafer. Each field's data was modeled using the lens-slit model. The contours plot the Wafer Bias offset of each slit exposure coefficient for each row on each field. The XY graph above the contours plots the magnitude of each coefficient as a function of its location on the wafer and therefore as a function of reticle-scan direction.

The upper graph of figure 12 is a population density plot. Population density is a box-plot that is plotted with the red data points being located at the median of the population. A typical box-plot figure is shown here for the first field on the plot for reference. Each field represents a different population with the quartiles extending from red to blue, blue being the first or fourth quartile. Points plotted as black-dots are the outliers of the box plot.

The data in figure 12 shows population medians that range from -5 to -7 in bias. Bias changes in roughly one nanometer increments depending upon the direction of the scan. Because this wafer was exposed using the same exposure tool as our previous example, the data continues to exhibit an overall tendency for bias to be higher in the last few exposure rows at the top of each field. This characteristic of the scanner was

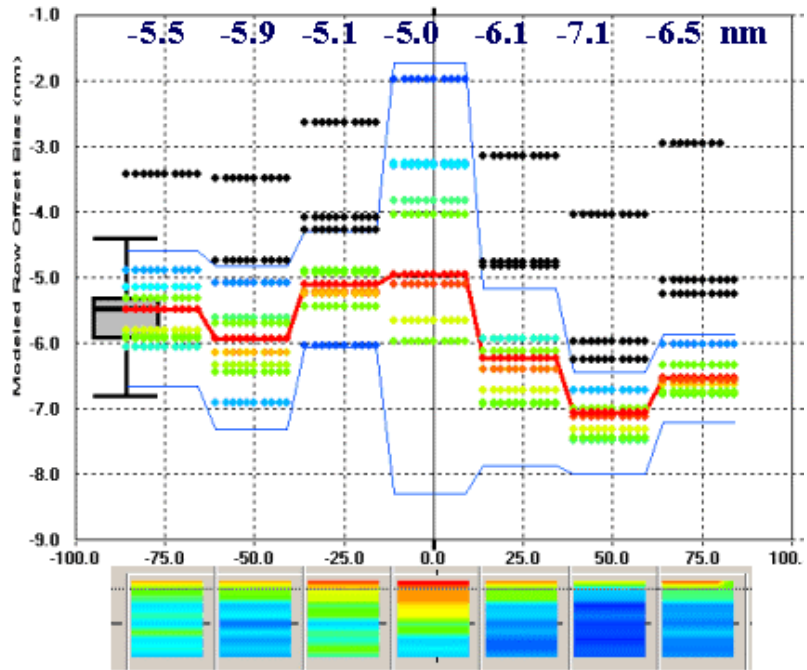


Figure 12: Bias change with scan direction for offset coefficient of row model.

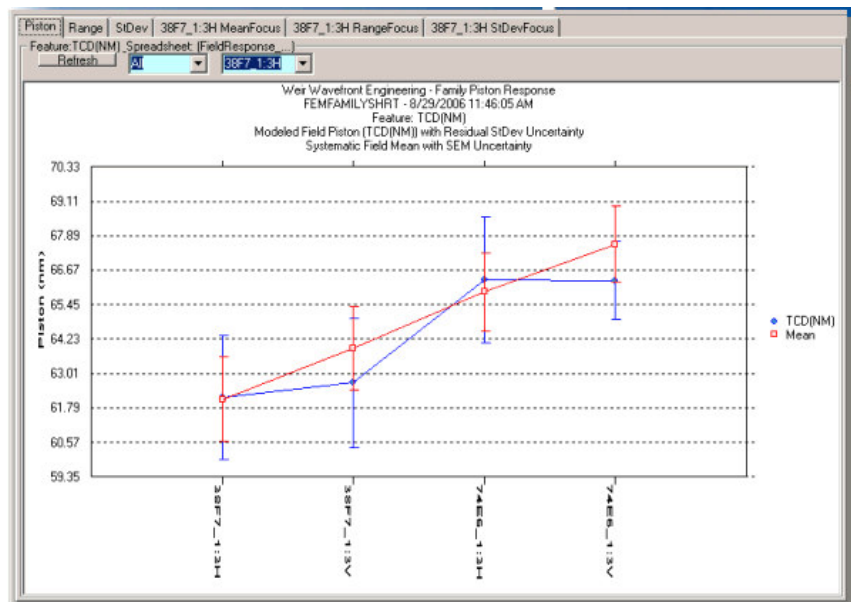


Figure 13: OPC evaluation for 65 nm, 1:3 Vertical & Horizontal features

presented in more detail in the discussion of figure 11 above.

The precision and detail that can be obtained using this technique is further presented in figure 13 for evaluation of different OPC structures. Two designs of a 65 nm feature designated “38F7” and “74E6” were selected for performance comparison across an FEM. These features are all for nested features in a 1:3 period. Vertical and horizontal orientation variants of each are presented.

The blue curve of Figure 13 presents the calculated offset coefficient for each design using the standard deviation of the residuals to this coefficient as the error bars. The vertical and horizontal feature offset coefficients for each design are equal within one nanometer showing the proper design image response. The 38F7 design provides a consistently smaller target across the FEM than the 74E6 design. The blue curve therefore tracks the design response for the OPC structure.

The red curve shows the average value of the feature with the vertical features being consistently larger by approximately 2 nm than their horizontal counterparts. The size difference in the mean-values of each image is caused by the spread of the exposure during scan and is an artifact of the exposure differences seen between vertical and horizontal oriented edges for a scanner.

## 10. Acknowledgements

We would like to thank Mircea Dusa of ASML Corporation for discussions on the data. We would also like to extend our gratitude to Hitachi and Nanometrics for their support and for allowing use of the data.

## 11. Conclusions

Full-field simulation platforms used in the design for manufacturing sequence currently support process window calibration to the target process to improve the accuracy of the simulations. Using the classic process window methodology to calibrate the simulation was shown to account for only two of the many sources of variation that is found in the perturbation spectrum of each semiconductor feature. The extrapolation of this technique to other profile variables such as film thickness was shown to result in even greater levels of approximation.

The reticle was shown to contain a perturbation signature that has a static component directly related to the feature sizes. Reticles with active elements such as phase shifting structures may also contain a dynamic component whose influence extends across the entire reticle and changes with the size of the feature and the conditions of exposure. The dynamic component of the reticle signature for a MoSiON reticle transfers into the image on the wafer and, in this data, was shown to contribute 4.5 nm of Wafer Bias perturbation

We next presented a method of deriving simulator calibrations by combining directly measured reticle signatures combined with modeling of the wafer image’s spatial characteristics. The static signature of the reticle was removed from wafer-image profile metrology of a focus exposure matrix to derive a data surface characterizing the change in Wafer Bias across each exposure field of the matrix. A field model designed to extract the spatial variation of wafer bias across each field was then applied to every exposure of the matrix. The coefficients of these models derive the control surface of systematic perturbations that defines the true response surface of the process. It was shown that perturbation signatures in this surface are stable and can be deconvolved to trace the disturbances back to their source.

Wafer Bias was shown to be dependent upon both dose and focus as is common knowledge in the industry. Not well known but obvious in simulation is that the range of Wafer Bias measured across each exposure field changes with focus and dose. This range minimizes at best focus and is asymmetric in its response to variations about the optimum focus. At optimum focus the field’s range of wafer bias is relatively constant over the exposures that are near and greater than the IsoFocal dose.

Wafer Bias varies across the field generating a well-defined spatial signature that is relatively constant within the process window. The signature is influenced by both the aberrations of the lens and by the scan-uniformity of the reticle stage. Reticle scan uniformity on this reticle was shown to contain a wafer bias of 5 nm near the top of the scan field. The direction of scan on the reticle was also shown to influence bias by one nanometer of variation for this dataset.

This improved technique of process window evaluation has been shown to be a valid analysis method for Wafer Bias calibration of process simulation tools. The method can also be extended to other evaluations including the characterization of optical proximity reticle structure design.

---

## 1. References

- 1 ) J. Hogan et al, "Design Process Optimization, Virtual Prototyping of Manufacturing & Foundry-portable DFM", Proc of SPIE (2006) vol. 5756-3
- 2) G. P. Hughes et al, "Study of OPC for AAPSM Reticles using various mask fabrication techniques", SPIE (2006), vol 5377-18
- 3 ) M. Dusa, T. Zavecz, R. Moerman, B. Singh, P. Friedberg, R.Hoobler, "Intra-wafer CDU characterization to determine process and focus contributions based on Scatterometry Metrology", Publications SPIE (2004) vol 5378-11
- 4) J. W. Bossung, "Projection Printing Characterization", Developments in Semiconductor Microlithography II, Proc. of SPIE(1977) Vol. 100, pp. 80-84
- 5 ) T. Zavecz, R. Hoobler, "Models for reticle performance and comparison of direct measurement", Proc. of SPIE (2005) vol. 5754-110
- 6 ) T. Zavecz, "Full-field feature profile models in process control", Proc of SPIE (2005), vol. 5755-16
- 7 ) T. Zavecz, "Bossung Curves; an old technique with a new twist for sub-90 nm nodes", Proc. of SPIE (2006) vol. 6152 - 109
- 8) W. Zhou, J.Yu, J. Lo, J. Liu, "Lithography process window analysis with calibrated model", Proc of SPIE (2004) 5375-29, pp. 721-726